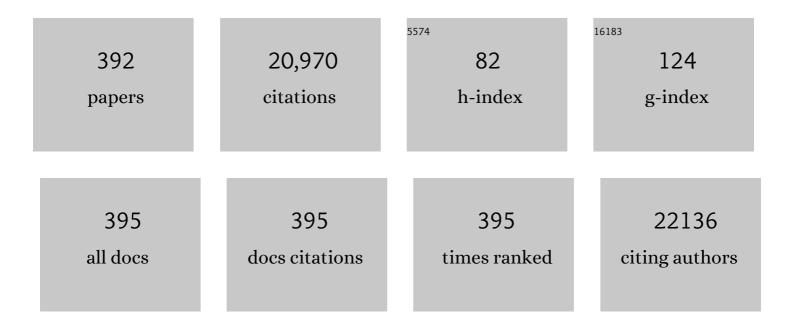
Yue Zhang

List of Publications by Year in descending order

Source: https://exaly.com/author-pdf/3321019/publications.pdf Version: 2024-02-01



YUE THANC

#	Article	IF	CITATIONS
1	Flexible and Highly Sensitive Strain Sensors Fabricated by Pencil Drawn for Wearable Monitor. Advanced Functional Materials, 2015, 25, 2395-2401.	14.9	439
2	Fabrication of a Highâ€Brightness Blueâ€Lightâ€Emitting Diode Using a ZnOâ€Nanowire Array Grown on pâ€GaN Thin Film. Advanced Materials, 2009, 21, 2767-2770.	21.0	425
3	Stretchableâ€Rubberâ€Based Triboelectric Nanogenerator and Its Application as Selfâ€Powered Body Motion Sensors. Advanced Functional Materials, 2015, 25, 3688-3696.	14.9	320
4	Toward the Application of High Frequency Electromagnetic Wave Absorption by Carbon Nanostructures. Advanced Science, 2019, 6, 1801057.	11.2	312
5	Evaluating the Stability of Co ₂ P Electrocatalysts in the Hydrogen Evolution Reaction for Both Acidic and Alkaline Electrolytes. ACS Energy Letters, 2018, 3, 1360-1365.	17.4	291
6	A highly shape-adaptive, stretchable design based on conductive liquid for energy harvesting and self-powered biomechanical monitoring. Science Advances, 2016, 2, e1501624.	10.3	274
7	Assembly of Ni(OH)2 nanoplates on reduced graphene oxide: a two dimensional nanocomposite for enzyme-free glucose sensing. Journal of Materials Chemistry, 2011, 21, 16949.	6.7	240
8	A Highly Stretchable ZnO@Fiberâ€Based Multifunctional Nanosensor for Strain/Temperature/UV Detection. Advanced Functional Materials, 2016, 26, 3074-3081.	14.9	239
9	High output piezoelectric nanocomposite generators composed of oriented BaTiO3 NPs@PVDF. Nano Energy, 2015, 11, 719-727.	16.0	237
10	A Flexible, Stretchable and Shapeâ€Adaptive Approach for Versatile Energy Conversion and Selfâ€Powered Biomedical Monitoring. Advanced Materials, 2015, 27, 3817-3824.	21.0	227
11	Ultraviolet Detectors Based on Wide Bandgap Semiconductor Nanowire: A Review. Sensors, 2018, 18, 2072.	3.8	222
12	Scanning Probe Study on the Piezotronic Effect in ZnO Nanomaterials and Nanodevices. Advanced Materials, 2012, 24, 4647-4655.	21.0	219
13	Ultrasensitive and stretchable resistive strain sensors designed for wearable electronics. Materials Horizons, 2017, 4, 502-510.	12.2	206
14	Secreted Frizzled-related protein 2 is a procollagen C proteinase enhancer with a role in fibrosis associated with myocardial infarction. Nature Cell Biology, 2009, 11, 46-55.	10.3	205
15	Thermoelectric Nanogenerators Based on Single Sb-Doped ZnO Micro/Nanobelts. ACS Nano, 2012, 6, 6984-6989.	14.6	199
16	Band alignment engineering for improved performance and stability of ZnFe2O4 modified CdS/ZnO nanostructured photoanode for PEC water splitting. Nano Energy, 2016, 24, 25-31.	16.0	196
17	Enhanced photoresponse of ZnO nanorods-based self-powered photodetector by piezotronic interface engineering. Nano Energy, 2014, 9, 237-244.	16.0	193
18	Poly(4-styrenesulfonate)-induced sulfur vacancy self-healing strategy for monolayer MoS2 homojunction photodiode. Nature Communications, 2017, 8, 15881.	12.8	191

#	Article	IF	CITATIONS
19	Stretchable and Waterproof Self-Charging Power System for Harvesting Energy from Diverse Deformation and Powering Wearable Electronics. ACS Nano, 2016, 10, 6519-6525.	14.6	182
20	Electromagnetic Shielding Hybrid Nanogenerator for Health Monitoring and Protection. Advanced Functional Materials, 2018, 28, 1703801.	14.9	178
21	3Dâ€Branched ZnO/CdS Nanowire Arrays for Solar Water Splitting and the Service Safety Research. Advanced Energy Materials, 2016, 6, 1501459.	19.5	177
22	Self-Powered Magnetic Sensor Based on a Triboelectric Nanogenerator. ACS Nano, 2012, 6, 10378-10383.	14.6	174
23	Harvesting Ambient Vibration Energy over a Wide Frequency Range for Self-Powered Electronics. ACS Nano, 2017, 11, 1728-1735.	14.6	169
24	The octa-twin tetraleg ZnO nanostructures. Solid State Communications, 2003, 126, 629-633.	1.9	167
25	Recent Advances in Triboelectric Nanogeneratorâ€Based Health Monitoring. Advanced Functional Materials, 2019, 29, 1808849.	14.9	167
26	Highly transparent triboelectric nanogenerator for harvesting water-related energy reinforced by antireflection coating. Scientific Reports, 2015, 5, 9080.	3.3	165
27	High—Performance Solarâ€Blind Deep Ultraviolet Photodetector Based on Individual Singleâ€Crystalline Zn ₂ GeO ₄ Nanowire. Advanced Functional Materials, 2016, 26, 704-712.	14.9	163
28	Selfâ€Powered Trajectory, Velocity, and Acceleration Tracking of a Moving Object/Body using a Triboelectric Sensor. Advanced Functional Materials, 2014, 24, 7488-7494.	14.9	161
29	Electromagnetic wave absorption in reduced graphene oxide functionalized with Fe3O4/Fe nanorings. Nano Research, 2016, 9, 2018-2025.	10.4	161
30	An innovative design of perovskite solar cells with Al 2 O 3 inserting at ZnO/perovskite interface for improving the performance and stability. Nano Energy, 2016, 22, 223-231.	16.0	157
31	Allâ€Inorganic Perovskite Quantum Dotâ€Monolayer MoS ₂ Mixedâ€Dimensional van der Waals Heterostructure for Ultrasensitive Photodetector. Advanced Science, 2018, 5, 1801219.	11.2	157
32	Directed Growth and Microwave Absorption Property of Crossed ZnO Netlike Micro-/Nanostructures. Journal of Physical Chemistry C, 2010, 114, 10088-10091.	3.1	154
33	Flexible and printable paper-based strain sensors for wearable and large-area green electronics. Nanoscale, 2016, 8, 13025-13032.	5.6	154
34	Investigation on the broadband electromagnetic wave absorption properties and mechanism of Co3O4-nanosheets/reduced-graphene-oxide composite. Nano Research, 2017, 10, 980-990.	10.4	154
35	Interface Engineering for Modulation of Charge Carrier Behavior in ZnO Photoelectrochemical Water Splitting. Advanced Functional Materials, 2019, 29, 1808032.	14.9	153
36	Flexible piezoelectric nanogenerators based on a fiber/ZnO nanowires/paper hybrid structure for energy harvesting. Nano Research, 2014, 7, 917-928.	10.4	152

#	Article	IF	CITATIONS
37	Novel Piezoelectric Paperâ€Based Flexible Nanogenerators Composed of BaTiO ₃ Nanoparticles and Bacterial Cellulose. Advanced Science, 2016, 3, 1500257.	11.2	152
38	Electronic Structure Engineering of Cu2O Film/ZnO Nanorods Array All-Oxide p-n Heterostructure for Enhanced Photoelectrochemical Property and Self-powered Biosensing Application. Scientific Reports, 2015, 5, 7882.	3.3	151
39	Structure and photocatalytic activity of Ni-doped ZnO nanorods. Materials Research Bulletin, 2011, 46, 1207-1210.	5.2	149
40	Size Dependence of Dielectric Constant in a Single Pencil-Like ZnO Nanowire. Nano Letters, 2012, 12, 1919-1922.	9.1	147
41	Bioinspired stretchable triboelectric nanogenerator as energy-harvesting skin for self-powered electronics. Nano Energy, 2017, 39, 429-436.	16.0	147
42	Nanopillar Arrayed Triboelectric Nanogenerator as a Self-Powered Sensitive Sensor for a Sleep Monitoring System. ACS Nano, 2016, 10, 8097-8103.	14.6	145
43	Self-Powered Photoelectrochemical Biosensor Based on CdS/RGO/ZnO Nanowire Array Heterostructure. Small, 2016, 12, 245-251.	10.0	142
44	Recyclable and Green Triboelectric Nanogenerator. Advanced Materials, 2017, 29, 1604961.	21.0	141
45	Self-powered ultraviolet photodetector based on a single Sb-doped ZnO nanobelt. Applied Physics Letters, 2010, 97, .	3.3	139
46	Bicrystalline zinc oxide nanowires. Chemical Physics Letters, 2003, 375, 96-101.	2.6	137
47	Enhanced photoelectrochemical property of ZnO nanorods array synthesized on reduced graphene oxide for self-powered biosensing application. Biosensors and Bioelectronics, 2015, 64, 499-504.	10.1	133
48	Green hybrid power system based on triboelectric nanogenerator for wearable/portable electronics. Nano Energy, 2019, 55, 151-163.	16.0	129
49	Self-Powered UV Photosensor Based on PEDOT:PSS/ZnO Micro/Nanowire with Strain-Modulated Photoresponse. ACS Applied Materials & amp; Interfaces, 2013, 5, 3671-3676.	8.0	128
50	Self-powered artificial electronic skin for high-resolution pressure sensing. Nano Energy, 2017, 32, 389-396.	16.0	125
51	Effect of Nb on hydrogen-induced delayed fracture in high strength hot stamping steels. Materials Science & Engineering A: Structural Materials: Properties, Microstructure and Processing, 2015, 626, 136-143.	5.6	121
52	Electret Film-Enhanced Triboelectric Nanogenerator Matrix for Self-Powered Instantaneous Tactile Imaging. ACS Applied Materials & Interfaces, 2014, 6, 3680-3688.	8.0	118
53	Grapheneâ€Based Mixedâ€Dimensional van der Waals Heterostructures for Advanced Optoelectronics. Advanced Materials, 2019, 31, e1806411.	21.0	115
54	Au-Embedded ZnO/NiO Hybrid with Excellent Electrochemical Performance as Advanced Electrode Materials for Supercapacitor. ACS Applied Materials & Interfaces, 2015, 7, 2480-2485.	8.0	114

#	Article	IF	CITATIONS
55	Carbon fiber–ZnO nanowire hybrid structures for flexible and adaptable strain sensors. Nanoscale, 2013, 5, 12350.	5.6	112
56	Development, applications, and future directions of triboelectric nanogenerators. Nano Research, 2018, 11, 2951-2969.	10.4	112
57	Flexible, Cuttable, and Self-Waterproof Bending Strain Sensors Using Microcracked Gold Nanofilms@Paper Substrate. ACS Applied Materials & Interfaces, 2017, 9, 4151-4158.	8.0	107
58	Interfacial Charge Behavior Modulation in Perovskite Quantum Dotâ€Monolayer MoS ₂ 0Dâ€2D Mixedâ€Dimensional van der Waals Heterostructures. Advanced Functional Materials, 2018, 28, 1802015.	14.9	107
59	Service Behavior of Multifunctional Triboelectric Nanogenerators. Advanced Materials, 2017, 29, 1606703.	21.0	106
60	Piezotronic Interface Engineering on ZnO/Au-Based Schottky Junction for Enhanced Photoresponse of a Flexible Self-Powered UV Detector. ACS Applied Materials & Interfaces, 2014, 6, 14116-14122.	8.0	105
61	Design of sandwich-structured ZnO/ZnS/Au photoanode for enhanced efficiency of photoelectrochemical water splitting. Nano Research, 2015, 8, 2891-2900.	10.4	104
62	X-ray photoelectron spectroscopic studies of Ba0.5Sr0.5Co0.8Fe0.2O3â^'δ cathode for solid oxide fuel cells. International Journal of Hydrogen Energy, 2009, 34, 435-439.	7.1	102
63	High On–Off Ratio Improvement of ZnO-Based Forming-Free Memristor by Surface Hydrogen Annealing. ACS Applied Materials & Interfaces, 2015, 7, 7382-7388.	8.0	102
64	Rootâ€specific NFâ€Y family transcription factor, <i>PdNFâ€YB21</i> , positively regulates root growth and drought resistance by abscisic acidâ€mediated indoylacetic acid transport in <i>Populu</i> s. New Phytologist, 2020, 227, 407-426.	7.3	102
65	Photoelectrochemical performance enhancement of ZnO photoanodes from ZnIn2S4 nanosheets coating. Nano Energy, 2015, 14, 392-400.	16.0	98
66	A self-powered ultraviolet photodetector based on solution-processed p-NiO/n-ZnO nanorod array heterojunction. RSC Advances, 2015, 5, 5976-5981.	3.6	97
67	Enhanced Efficiency and Stability of Perovskite Solar Cells via Anti-Solvent Treatment in Two-Step Deposition Method. ACS Applied Materials & Interfaces, 2017, 9, 7224-7231.	8.0	97
68	In situmechanical properties of individual ZnO nanowires and the mass measurement of nanoparticles. Journal of Physics Condensed Matter, 2006, 18, L179-L184.	1.8	96
69	Performance and service behavior in 1-D nanostructured energy conversion devices. Nano Energy, 2015, 14, 30-48.	16.0	96
70	Temperature-dependent electrochemical capacitive performance of the α-Fe2O3 hollow nanoshuttles as supercapacitor electrodes. Journal of Colloid and Interface Science, 2016, 466, 291-296.	9.4	94
71	An Amphiphobic Hydraulic Triboelectric Nanogenerator for a Selfâ€Cleaning and Selfâ€Charging Power System. Advanced Functional Materials, 2018, 28, 1803117.	14.9	94
72	Strain-Engineered van der Waals Interfaces of Mixed-Dimensional Heterostructure Arrays. ACS Nano, 2019, 13, 9057-9066.	14.6	94

#	Article	IF	CITATIONS
73	Defectâ€Engineered Atomically Thin MoS ₂ Homogeneous Electronics for Logic Inverters. Advanced Materials, 2020, 32, e1906646.	21.0	94
74	Enzyme-coated single ZnO nanowire FET biosensor for detection of uric acid. Sensors and Actuators B: Chemical, 2013, 176, 22-27.	7.8	93
75	Enhanced photoresponse of Cu2O/ZnO heterojunction with piezo-modulated interface engineering. Nano Research, 2014, 7, 860-868.	10.4	93
76	Kelvin probe force microscopy for perovskite solar cells. Science China Materials, 2019, 62, 776-789.	6.3	93
77	Improved Photoresponse Performance of Self-Powered ZnO/Spiro-MeOTAD Heterojunction Ultraviolet Photodetector by Piezo-Phototronic Effect. ACS Applied Materials & Interfaces, 2016, 8, 6137-6143.	8.0	92
78	Self-powered photoelectrochemical biosensing platform based on Au NPs@ZnO nanorods array. Nano Research, 2016, 9, 344-352.	10.4	92
79	Integrated multi-unit transparent triboelectric nanogenerator harvesting rain power for driving electronics. Nano Energy, 2016, 25, 18-25.	16.0	91
80	Advent of alkali metal doping: a roadmap for the evolution of perovskite solar cells. Chemical Society Reviews, 2021, 50, 2696-2736.	38.1	90
81	Oxygen reduction mechanism at Ba0.5Sr0.5Co0.8Fe0.2O3â^î́r cathode for solid oxide fuel cell. International Journal of Hydrogen Energy, 2009, 34, 1008-1014.	7.1	87
82	Gold nanoparticle/ZnO nanorod hybrids for enhanced reactive oxygen species generation and photodynamic therapy. Nano Research, 2015, 8, 2004-2014.	10.4	85
83	Strain Modulation in Graphene/ZnO Nanorod Film Schottky Junction for Enhanced Photosensing Performance. Advanced Functional Materials, 2016, 26, 1347-1353.	14.9	85
84	ZnO nanowire array ultraviolet photodetectors with self-powered properties. Current Applied Physics, 2013, 13, 165-169.	2.4	81
85	Formation of double-side teethed nanocombs of ZnO and self-catalysis of Zn-terminated polar surface. Chemical Physics Letters, 2006, 417, 358-362.	2.6	80
86	Strain Engineering in 2D Materialâ€Based Flexible Optoelectronics. Small Methods, 2021, 5, e2000919.	8.6	80
87	Structure effect on graphene-modified enzyme electrode glucose sensors. Biosensors and Bioelectronics, 2014, 52, 281-287.	10.1	78
88	Field Emission of a Single In-Doped ZnO Nanowire. Journal of Physical Chemistry C, 2007, 111, 9039-9043.	3.1	76
89	Functional triboelectric generator as self-powered vibration sensor with contact mode and non-contact mode. Nano Energy, 2015, 14, 209-216.	16.0	76
90	Cactus-like hierarchical nanorod-nanosheet mixed dimensional photoanode for efficient and stable water splitting. Nano Energy, 2017, 35, 189-198.	16.0	76

Yue Zhang

#	Article	IF	CITATIONS
91	Fibronectin Binds and Enhances the Activity of Bone Morphogenetic Protein 1. Journal of Biological Chemistry, 2009, 284, 25879-25888.	3.4	74
92	Three-Dimensional Ordered ZnO/Cu ₂ 0 Nanoheterojunctions for Efficient Metal–Oxide Solar Cells. ACS Applied Materials & Interfaces, 2015, 7, 3216-3223.	8.0	74
93	Improvement of the performance of dye-sensitized solar cells using Sn-doped ZnO nanoparticles. Journal of Power Sources, 2010, 195, 5806-5809.	7.8	73
94	Lignin–phenol–formaldehyde resin adhesives prepared with biorefinery technical lignins. Journal of Applied Polymer Science, 2015, 132, .	2.6	72
95	The ability of MLL to bind RUNX1 and methylate H3K4 at PU.1 regulatory regions is impaired by MDS/AML-associated RUNX1/AML1 mutations. Blood, 2011, 118, 6544-6552.	1.4	71
96	A three-dimensional reticulate CNT-aerogel for a high mechanical flexibility fiber supercapacitor. Nanoscale, 2018, 10, 9360-9368.	5.6	71
97	Improved glucose electrochemical biosensor by appropriate immobilization of nano-ZnO. Colloids and Surfaces B: Biointerfaces, 2011, 82, 168-172.	5.0	70
98	Enhanced Performance of ZnO Piezotronic Pressure Sensor through Electron-Tunneling Modulation of MgO Nanolayer. ACS Applied Materials & amp; Interfaces, 2015, 7, 1602-1607.	8.0	70
99	Investigation on the optimization, design and microwave absorption properties of reduced graphene oxide/tetrapod-like ZnO composites. RSC Advances, 2015, 5, 10197-10203.	3.6	70
100	ZnO nanostructures in enzyme biosensors. Science China Materials, 2015, 58, 60-76.	6.3	70
101	Fiber-shaped asymmetric supercapacitors with ultrahigh energy density for flexible/wearable energy storage. Journal of Materials Chemistry A, 2016, 4, 17704-17710.	10.3	69
102	Self-Healing Originated van der Waals Homojunctions with Strong Interlayer Coupling for High-Performance Photodiodes. ACS Nano, 2019, 13, 3280-3291.	14.6	69
103	Morphology, structures and properties of ZnO nanobelts fabricated by Zn-powder evaporation without catalyst at lower temperature. Journal of Materials Science, 2006, 41, 3057-3062.	3.7	68
104	Synergistic Effect of Surface Plasmonic particles and Surface Passivation layer on ZnO Nanorods Array for Improved Photoelectrochemical Water Splitting. Scientific Reports, 2016, 6, 29907.	3.3	68
105	Phase reconfiguration of multivalent nickel sulfides in hydrogen evolution. Energy and Environmental Science, 2022, 15, 633-644.	30.8	68
106	A highly sensitive electrochemical biosensor based on zinc oxide nanotetrapods for l-lactic acid detection. Nanoscale, 2012, 4, 3438.	5.6	67
107	Uniformly assembled vanadium doped ZnO microflowers/ bacterial cellulose hybrid paper for flexible piezoelectric nanogenerators and self-powered sensors. Nano Energy, 2018, 52, 501-509.	16.0	67
108	Nonenzymatic Glucose Sensor Based on In Situ Reduction of Ni/NiO-Graphene Nanocomposite. Sensors, 2016, 16, 1791.	3.8	66

Yue Zhang

#	Article	IF	CITATIONS
109	Piezotronic effect on interfacial charge modulation in mixed-dimensional Van der Waals heterostructure for ultrasensitive flexible photodetectors. Nano Energy, 2019, 58, 85-93.	16.0	66
110	Highly sensitive uric acid biosensor based on individual zinc oxide micro/nanowires. Mikrochimica Acta, 2013, 180, 759-766.	5.0	65
111	Controllable fabrication and electromechanical characterization of single crystalline Sb-doped ZnO nanobelts. Applied Physics Letters, 2008, 92, .	3.3	63
112	Selfâ€Recovering Triboelectric Nanogenerator as Active Multifunctional Sensors. Advanced Functional Materials, 2015, 25, 6489-6494.	14.9	63
113	Emerging Conductive Atomic Force Microscopy for Metal Halide Perovskite Materials and Solar Cells. Advanced Energy Materials, 2020, 10, 1903922.	19.5	63
114	In Situ Transmission Electron Microscopy Investigation on Fatigue Behavior of Single ZnO Wires under High-Cycle Strain. Nano Letters, 2014, 14, 480-485.	9.1	62
115	Microwave absorption properties of carbon nanotubes and tetrapod-shaped ZnO nanostructures composites. Materials Science and Engineering B: Solid-State Materials for Advanced Technology, 2010, 175, 81-85.	3.5	61
116	Highly efficient piezotronic strain sensors with symmetrical Schottky contacts on the monopolar surface of ZnO nanobelts. Nanoscale, 2015, 7, 1796-1801.	5.6	60
117	The enhanced performance of piezoelectric nanogenerator via suppressing screening effect with Au particles/ZnO nanoarrays Schottky junction. Nano Research, 2016, 9, 372-379.	10.4	60
118	Synthesis and Characterization of Sb-Doped ZnO Nanobelts with Single-Side Zigzag Boundaries. Journal of Physical Chemistry C, 2008, 112, 17916-17919.	3.1	59
119	Oxidation of zirconium diboride–silicon carbide ceramics under an oxygen partial pressure of 200 Pa: Formation of zircon. Corrosion Science, 2010, 52, 3297-3303.	6.6	59
120	Layer Dependence and Light Tuning Surface Potential of 2D MoS ₂ on Various Substrates. Small, 2017, 13, 1603103.	10.0	58
121	Self-powered flexible antibacterial tactile sensor based on triboelectric-piezoelectric-pyroelectric multi-effect coupling mechanism. Nano Energy, 2019, 66, 104105.	16.0	58
122	Functional nanogenerators as vibration sensors enhanced by piezotronic effects. Nano Research, 2014, 7, 190-198.	10.4	56
123	Simulation and structure optimization of triboelectric nanogenerators considering the effects of parasitic capacitance. Nano Research, 2017, 10, 157-171.	10.4	56
124	High-performance piezoelectric gate diode of a single polar-surface dominated ZnO nanobelt. Nanotechnology, 2009, 20, 125201.	2.6	55
125	Disordered epigenetic regulation in MLL-related leukemia. International Journal of Hematology, 2012, 96, 428-437.	1.6	55
126	A self-powered ultraviolet detector based on a single ZnO microwire/p-Si film with double heterojunctions. Nanoscale, 2014, 6, 6025-6029.	5.6	55

#	Article	IF	CITATIONS
127	Double-Shelled Co ₃ O ₄ /C Nanocages Enabling Polysulfides Adsorption for High-Performance Lithium–Sulfur Batteries. ACS Applied Energy Materials, 2019, 2, 8153-8162.	5.1	55
128	High Performance Indium-Doped ZnO Gas Sensor. Journal of Nanomaterials, 2015, 2015, 1-6.	2.7	54
129	Ultralight, self-powered and self-adaptive motion sensor based on triboelectric nanogenerator for perceptual layer application in Internet of things. Nano Energy, 2018, 48, 312-319.	16.0	54
130	3D architecture of a graphene/CoMoO4 composite for asymmetric supercapacitors usable at various temperatures. Journal of Colloid and Interface Science, 2017, 493, 42-50.	9.4	53
131	Flexible piezoresistive strain sensor based on single Sb-doped ZnO nanobelts. Applied Physics Letters, 2010, 97, 223107.	3.3	52
132	Reduced Graphene Oxide Functionalized with Cobalt Ferrite Nanocomposites for Enhanced Efficient and Lightweight Electromagnetic Wave Absorption. Scientific Reports, 2016, 6, 32381.	3.3	52
133	Self-powered ultrasensitive pulse sensors for noninvasive multi-indicators cardiovascular monitoring. Nano Energy, 2021, 81, 105614.	16.0	52
134	ZnO Nanotubes Grown at Low Temperature Using Ga as Catalysts and Their Enhanced Photocatalytic Activities. Journal of Physical Chemistry C, 2009, 113, 10379-10383.	3.1	51
135	Ba0.5Sr0.5Co0.8Fe0.2O3 nanopowders prepared by glycine–nitrate process for solid oxide fuel cell cathode. Journal of Alloys and Compounds, 2008, 453, 418-422.	5.5	50
136	Raman spectra and photoluminescence properties of In-doped ZnO nanostructures. Materials Letters, 2010, 64, 569-572.	2.6	50
137	<i>PdGNC</i> confers drought tolerance by mediating stomatal closure resulting from NO and H ₂ O ₂ production via the direct regulation of <i>PdHXK1</i> expression in <i>Populus</i> . New Phytologist, 2021, 230, 1868-1882.	7.3	50
138	Tumbler-shaped hybrid triboelectric nanogenerators for amphibious self-powered environmental monitoring. Nano Energy, 2020, 76, 104960.	16.0	49
139	Microwave absorption properties of carbon black and tetrapod-like ZnO whiskers composites. Applied Surface Science, 2013, 286, 7-11.	6.1	48
140	Self-powered ultraviolet photodetectors based on selectively grown ZnO nanowire arrays with thermal tuning performance. Physical Chemistry Chemical Physics, 2014, 16, 9525.	2.8	48
141	Structure and photoluminescence of S-doped ZnO nanorod arrays. Materials Letters, 2009, 63, 444-446.	2.6	47
142	ZnO nanotetrapod network as the adsorption layer for the improvement of glucose detection via multiterminal electron-exchange. Colloids and Surfaces A: Physicochemical and Engineering Aspects, 2010, 361, 169-173.	4.7	47
143	V ₂ O ₅ Nanowire Composite Paper as a High-Performance Lithium-Ion Battery Cathode. ACS Omega, 2017, 2, 793-799.	3.5	46
144	Oxidation behaviour of zirconium diboride–silicon carbide ceramic composites under low oxygen partial pressure. Corrosion Science, 2011, 53, 3742-3746.	6.6	45

#	Article	IF	CITATIONS
145	Simple fabrication of a ZnO nanorod array UV detector with a high performance. Physica E: Low-Dimensional Systems and Nanostructures, 2014, 61, 180-184.	2.7	45
146	Boosting the Sensitivity of a Photoelectrochemical Immunoassay by Using SiO ₂ @polydopamine Core–Shell Nanoparticles as a Highly Efficient Quencher. ACS Applied Nano Materials, 2019, 2, 1579-1588.	5.0	45
147	Atomicâ€Thin ZnO Sheet for Visibleâ€Blind Ultraviolet Photodetection. Small, 2020, 16, e2005520.	10.0	45
148	Longitudinal effects of air pollution on exhaled nitric oxide: the Children's Health Study. Occupational and Environmental Medicine, 2014, 71, 507-513.	2.8	44
149	Large-scale patterned ZnO nanorod arrays for efficient photoelectrochemical water splitting. Applied Surface Science, 2015, 339, 122-127.	6.1	44
150	Transverse piezoelectric field-effect transistor based on single ZnO nanobelts. Physical Chemistry Chemical Physics, 2010, 12, 12415.	2.8	43
151	Bioinspired Tribotronic Resistive Switching Memory for Self-Powered Memorizing Mechanical Stimuli. ACS Applied Materials & Interfaces, 2017, 9, 43822-43829.	8.0	42
152	Low-voltage blue light emission from n-ZnO/p-GaN heterojunction formed by RF magnetron sputtering method. Current Applied Physics, 2014, 14, 345-348.	2.4	41
153	Strain modulation on graphene/ZnO nanowire mixed-dimensional van der Waals heterostructure for high-performance photosensor. Nano Research, 2017, 10, 3476-3485.	10.4	41
154	3D Holeyâ€Graphene Architecture Expedites Ion Transport Kinetics to Push the OER Performance. Advanced Energy Materials, 2020, 10, 2001005.	19.5	41
155	Ion migration in hybrid perovskites: Classification, identification, and manipulation. Nano Today, 2022, 44, 101503.	11.9	41
156	Doping and defects in the formation of single-crystal ZnO nanodisks. Applied Physics Letters, 2006, 89, 252115.	3.3	40
157	Oxidation behavior of SiC–SiBCN ceramics. Ceramics International, 2015, 41, 1023-1030.	4.8	40
158	A Stress-Responsive NAC Transcription Factor from Tiger Lily (LINAC2) Interacts with LIDREB1 and LIZHFD4 and Enhances Various Abiotic Stress Tolerance in Arabidopsis. International Journal of Molecular Sciences, 2019, 20, 3225.	4.1	40
159	Ligand Engineering for Improved Allâ€Inorganic Perovskite Quantum Dotâ€MoS ₂ Monolayer Mixed Dimensional van der Waals Phototransistor. Small Methods, 2019, 3, 1900117.	8.6	40
160	A stretching-insensitive, self-powered and wearable pressure sensor. Nano Energy, 2022, 91, 106695.	16.0	40
161	Synthesis and characterization of Zn1â^'xMnxO nanowires. Applied Physics Letters, 2008, 92, .	3.3	39
162	Multi-unit hydroelectric generator based on contact electrification and its service behavior. Nano Energy, 2015, 16, 329-338.	16.0	39

#	Article	IF	CITATIONS
163	Integrated hybrid nanogenerator for gas energy recycle and purification. Nano Energy, 2017, 39, 524-531.	16.0	39
164	Design of efficient dye-sensitized solar cells with patterned ZnO–ZnS core–shell nanowire array photoanodes. Nanoscale, 2014, 6, 4691-4697.	5.6	38
165	Enhanced power conversion efficiency of CdS quantum dot sensitized solar cells with ZnO nanowire arrays as the photoanodes. Optics Communications, 2015, 349, 198-202.	2.1	38
166	Valorization of lignin and cellulose in acid-steam-exploded corn stover by a moderate alkaline ethanol post-treatment based on an integrated biorefinery concept. Biotechnology for Biofuels, 2016, 9, 238.	6.2	38
167	Facile synthesis of NiCo2S4 nanowire arrays on 3D graphene foam for high-performance electrochemical capacitors application. Journal of Materials Science, 2018, 53, 10292-10301.	3.7	38
168	Pathobiological Pseudohypoxia as a Putative Mechanism Underlying Myelodysplastic Syndromes. Cancer Discovery, 2018, 8, 1438-1457.	9.4	38
169	Gateâ€Controlled Polarityâ€Reversible Photodiodes with Ambipolar 2D Semiconductors. Advanced Functional Materials, 2021, 31, 2007559.	14.9	38
170	Facile synthesis of highly uniform Mn/Co-codoped ZnO nanowires: Optical, electrical, and magnetic properties. Nanoscale, 2011, 3, 654-660.	5.6	37
171	A facile method for the preparation of three-dimensional CNT sponge and a nanoscale engineering design for high performance fiber-shaped asymmetric supercapacitors. Journal of Materials Chemistry A, 2017, 5, 22559-22567.	10.3	37
172	Fabrication and characterization of ZnO comb-like nanostructures. Ceramics International, 2006, 32, 561-566.	4.8	36
173	Effect of hydrothermal reaction temperature on growth, photoluminescence and photoelectrochemical properties of ZnO nanorod arrays. Materials Chemistry and Physics, 2010, 123, 811-815.	4.0	36
174	Reduced Graphene Oxideâ€Functionalized High Electron Mobility Transistors for Novel Recognition Pattern Labelâ€Free DNA Sensors. Small, 2013, 9, 4045-4050.	10.0	36
175	Coupling metal-organic framework nanosphere and nanobody for boosted photoelectrochemical immunoassay of Human Epididymis Protein 4. Analytica Chimica Acta, 2020, 1107, 145-154.	5.4	36
176	CuNiO nanoparticles assembled on graphene as an effective platform for enzyme-free glucose sensing. Analytica Chimica Acta, 2015, 858, 49-54.	5.4	35
177	Influence of carrier concentration on the resistive switching characteristics of a ZnO-based memristor. Nano Research, 2016, 9, 1116-1124.	10.4	35
178	Stability of CoP _{<i>x</i>} Electrocatalysts in Continuous and Interrupted Acidic Electrolysis of Water. ChemElectroChem, 2018, 5, 1230-1239.	3.4	35
179	Low-Temperature Phase-Controlled Synthesis of Titanium Di- and Tri-sulfide by Atomic Layer Deposition. Chemistry of Materials, 2019, 31, 9354-9362.	6.7	35
180	La0.9Sr0.1Ga0.8Mg0.2O3â^'δ sintered by spark plasma sintering (SPS) for intermediate temperature SOFC electrolyte. Journal of Alloys and Compounds, 2008, 458, 383-389.	5.5	34

#	Article	IF	CITATIONS
181	Electrical breakdown of ZnO nanowires in metal-semiconductor-metal structure. Applied Physics Letters, 2010, 96, .	3.3	34
182	Design and tailoring of patterned ZnO nanostructures for energy conversion applications. Science China Materials, 2017, 60, 793-810.	6.3	34
183	Stress hematopoiesis reveals abnormal control of self-renewal, lineage bias, and myeloid differentiation in Mll partial tandem duplication (Mll-PTD) hematopoietic stem/progenitor cells. Blood, 2012, 120, 1118-1129.	1.4	32
184	A tunable ZnO/electrolyte heterojunction for a self-powered photodetector. Physical Chemistry Chemical Physics, 2014, 16, 26697-26700.	2.8	32
185	Strain-modulation and service behavior of Au–MgO–ZnO ultraviolet photodetector by piezo-phototronic effect. Nano Research, 2015, 8, 3772-3779.	10.4	32
186	Cold nanoparticles coated zinc oxide nanorods as the matrix for enhanced l-lactate sensing. Colloids and Surfaces B: Biointerfaces, 2015, 126, 476-480.	5.0	32
187	Mapping the scientific research on non-point source pollution: a bibliometric analysis. Environmental Science and Pollution Research, 2017, 24, 4352-4366.	5.3	32
188	Self-catalytic Synthesis, Structures, and Properties of High-Quality Tetrapod-Shaped ZnO Nanostructures. Crystal Growth and Design, 2009, 9, 1863-1868.	3.0	31
189	ZnO nano-array-based EGFET biosensor for glucose detection. Applied Physics A: Materials Science and Processing, 2015, 119, 807-811.	2.3	31
190	Thermal properties and morphology of recycled poly(ethylene terephthalate)/maleic anhydride grafted linear lowâ€density polyethylene blends. Journal of Applied Polymer Science, 2008, 109, 3546-3553.	2.6	30
191	A self-powered strain senor based on a ZnO/PEDOT:PSS hybrid structure. RSC Advances, 2013, 3, 17011.	3.6	30
192	Saturated blue-violet electroluminescence from single ZnO micro/nanowire and p-GaN film hybrid light-emitting diodes. Applied Physics Letters, 2013, 102, .	3.3	29
193	Bias-tunable dual-mode ultraviolet photodetectors for photoelectric tachometer. Applied Physics Letters, 2014, 104, .	3.3	29
194	Downregulation of RUNX1/CBFβ by MLL fusion proteins enhances hematopoietic stem cell self-renewal. Blood, 2014, 123, 1729-1738.	1.4	29
195	Substrate-independent and large-area synthesis of carbon nanotube thin films using ZnO nanorods as template and dopamine as carbon precursor. Carbon, 2015, 83, 275-281.	10.3	29
196	Stabilization effects in binary colloidal Cu and Ag nanoparticle electrodes under electrochemical CO ₂ reduction conditions. Nanoscale, 2021, 13, 4835-4844.	5.6	29
197	Interpretation of Rubidiumâ€Based Perovskite Recipes toward Electronic Passivation and Ionâ€Diffusion Mitigation. Advanced Materials, 2022, 34, e2109998.	21.0	29
198	Single-Stranded DNA Functionalized Single-Walled Carbon Nanotubes for Microbiosensors via Layer-by-Layer Electrostatic Self-Assembly. ACS Applied Materials & Interfaces, 2014, 6, 3784-3789.	8.0	28

#	Article	IF	CITATIONS
199	High sensitivity, fast speed and self-powered ultraviolet photodetectors based on ZnO micro/nanowire networks. Progress in Natural Science: Materials International, 2014, 24, 1-5.	4.4	28
200	Graphdiyne Nanowall for Enhanced Photoelectrochemical Performance of Si Heterojunction Photoanode. ACS Applied Materials & amp; Interfaces, 2019, 11, 2745-2749.	8.0	28
201	Effects of different types of polyethylene on the morphology and properties of recycled poly(ethylene) Tj ETQq1 1 1851-1858.	0.784314 3.2	4 rgBT /Ove 27
202	Size effect in a cantilevered ZnO micro/nanowire and its potential as a performance tunable force sensor. RSC Advances, 2013, 3, 19375.	3.6	27
203	Preparation and Characterization of Lignocellulosic Oil Sorbent by Hydrothermal Treatment of Populus Fiber. Materials, 2014, 7, 6733-6747.	2.9	27
204	Zinc oxide nanowires-based electrochemical biosensor for L-lactic acid amperometric detection. Journal of Nanoparticle Research, 2014, 16, 1.	1.9	27
205	Influence of the carrier concentration on the piezotronic effect in a ZnO/Au Schottky junction. Nanoscale, 2015, 7, 4461-4467.	5.6	27
206	Ferroelectric polarization-enhanced charge separation in a vanadium-doped ZnO photoelectrochemical system. Inorganic Chemistry Frontiers, 2018, 5, 1533-1539.	6.0	27
207	An enzyme cascade-based electrochemical immunoassay using a polydopamine–carbon nanotube nanocomposite for signal amplification. Journal of Materials Chemistry B, 2018, 6, 8180-8187.	5.8	27
208	Interface Engineering in 1D ZnOâ€Based Heterostructures for Photoelectrical Devices. Advanced Functional Materials, 2022, 32, 2106887.	14.9	27
209	Mammalian Tolloid-like 1 Binds Procollagen C-proteinase Enhancer Protein 1 and Differs from Bone Morphogenetic Protein 1 in the Functional Roles of Homologous Protein Domains. Journal of Biological Chemistry, 2006, 281, 10786-10798.	3.4	26
210	Ptlr/ZnO nanowire/pentacene hybrid back-to-back double diodes. Applied Physics Letters, 2008, 93, 133101.	3.3	26
211	Oxidation kinetics of hot-pressed ZrB2–SiC ceramic matrix composites. Ceramics International, 2013, 39, 3113-3119.	4.8	26
212	Impact of climate change and drought regime on water footprint of crop production: the case of Lake Dianchi Basin, China. Natural Hazards, 2015, 79, 549-566.	3.4	26
213	Size dependence and UV irradiation tuning of the surface potential in single conical ZnO nanowires. RSC Advances, 2015, 5, 42075-42080.	3.6	26
214	High carrier concentration ZnO nanowire arrays for binder-free conductive support of supercapacitors electrodes by Al doping. Journal of Colloid and Interface Science, 2016, 484, 155-161.	9.4	26
215	Explosive field emission and plasma expansion of carbon nanotube cathodes. Applied Physics Letters, 2007, 90, 151504.	3.3	25
216	Electrical bistability and negative differential resistance in single Sb-doped ZnO nanobelts/SiOx/p-Si heterostructured devices. Applied Physics Letters, 2010, 96, .	3.3	25

#	Article	IF	CITATIONS
217	Mechanical and longitudinal electromechanical properties of Sb-doped ZnO nanobelts. CrystEngComm, 2010, 12, 2005.	2.6	25
218	Electronic transport properties of In-doped ZnO nanobelts with different concentration. Nanoscale, 2011, 3, 2182.	5.6	25
219	Self-powered ultraviolet photodetector based on a single ZnO tetrapod/PEDOT:PSS heterostructure. Semiconductor Science and Technology, 2013, 28, 105023.	2.0	25
220	Band alignment engineering for high-energy-density solid-state asymmetric supercapacitors with TiO ₂ insertion at the ZnO/Ni(OH) ₂ interface. Journal of Materials Chemistry A, 2016, 4, 17981-17987.	10.3	25
221	A MYB-Related Transcription Factor from Lilium lancifolium L. (LIMYB3) Is Involved in Anthocyanin Biosynthesis Pathway and Enhances Multiple Abiotic Stress Tolerance in Arabidopsis thaliana. International Journal of Molecular Sciences, 2019, 20, 3195.	4.1	25
222	Hemicyanine-based near-infrared fluorescent probe for the ultrasensitive detection of hNQO1 activity and discrimination ofÂhuman cancer cells. Analytica Chimica Acta, 2019, 1090, 125-132.	5.4	25
223	Multicenter Uric Acid Biosensor Based on Tetrapod-Shaped ZnO Nanostructures. Journal of Nanoscience and Nanotechnology, 2012, 12, 513-518.	0.9	24
224	An excellent enzymatic lactic acid biosensor with ZnO nanowires-gated AlGaAs/GaAs high electron mobility transistor. Nanoscale, 2012, 4, 6415.	5.6	24
225	Ultraviolet and visible photoresponse properties of a ZnO/Si heterojunction at zero bias. RSC Advances, 2013, 3, 17682.	3.6	24
226	Integrated active sensor system for real time vibration monitoring. Scientific Reports, 2015, 5, 16063.	3.3	23
227	Effect of carrier screening on ZnO-based resistive switching memory devices. Nano Research, 2017, 10, 77-86.	10.4	23
228	Synergistic engineering of dielectric and magnetic losses in M-Co/RGO nanocomposites for use in high-performance microwave absorption. Materials Chemistry Frontiers, 2020, 4, 3013-3021.	5.9	23
229	Doping Effect on High-Pressure Structural Stability of ZnO Nanowires. Journal of Physical Chemistry C, 2009, 113, 1164-1167.	3.1	22
230	Facile synthesis and photoelectrochemical performance of the bush-like ZnO nanosheets film. Solid State Sciences, 2012, 14, 155-158.	3.2	22
231	Preparation and anti-oxidation characteristics of ZrSiO4–SiBCN(O) amorphous coating. Applied Surface Science, 2015, 331, 490-496.	6.1	22
232	Nanorod arrays composed of zinc oxide modified with gold nanoparticles and glucose oxidase for enzymatic sensing of glucose. Mikrochimica Acta, 2015, 182, 605-610.	5.0	22
233	Structural dependence of piezoelectric size effects and macroscopic polarization in ZnO nanowires: A first-principles study. Nano Research, 2015, 8, 2073-2081.	10.4	22
234	Carbon Quantum Dots Decorated C ₃ N ₄ /TiO ₂ Heterostructure Nanorod Arrays for Enhanced Photoelectrochemical Performance. Journal of the Electrochemical Society, 2017, 164, H515-H520.	2.9	22

#	Article	IF	CITATIONS
235	In situ microscopy techniques for characterizing the mechanical properties and deformation behavior of two-dimensional (2D) materials. Materials Today, 2021, 51, 247-272.	14.2	22
236	A novel logic switch based on individual ZnO nanotetrapods. Nanoscale, 2011, 3, 2166.	5.6	21
237	Electrically pumped lasing from single ZnO micro/nanowire and poly(3,4-ethylenedioxythiophene):poly(styrenexulfonate) hybrid heterostructures. Applied Physics Letters, 2012, 101, 043119.	3.3	21
238	Analysis of Influencing Factors of Water Footprint Based on the STIRPAT Model: Evidence from the Beijing Agricultural Sector. Water (Switzerland), 2016, 8, 513.	2.7	21
239	A rationally designed output current measurement procedure and comprehensive understanding of the output characteristics for piezoelectric nanogenerators. Nano Energy, 2016, 30, 180-186.	16.0	21
240	Low-cost highly sensitive strain sensors for wearable electronics. Journal of Materials Chemistry C, 2017, 5, 10571-10577.	5.5	21
241	In-doped zinc oxide dodecagonal nanometer thick disks. Materials Letters, 2006, 60, 2623-2626.	2.6	20
242	Growth mechanism and optical properties of ZnS nanotetrapods. Nanotechnology, 2007, 18, 475603.	2.6	20
243	Characteristics of Ba0.5Sr0.5Co0.8Fe0.2O3â ^{~°} δ–La0.9Sr0.1Ga0.8Mg0.2O3â ^{~°} δ composite cathode for solid oxide fuel cell. Journal of Power Sources, 2008, 175, 189-195.	7.8	20
244	Preparation and characterization of La0.9Sr0.1Ga0.8Mg0.2O3â~δthin film on the porous cathode for SOFC. International Journal of Hydrogen Energy, 2009, 34, 440-445.	7.1	20
245	Walnut Polyphenol Extract Protects against Fenitrothion-Induced Immunotoxicity in Murine Splenic Lymphocytes. Nutrients, 2018, 10, 1838.	4.1	20
246	Endogenous Synergistic Enhanced Selfâ€Powered Photodetector via Multiâ€Effect Coupling Strategy toward Highâ€Efficiency Ultraviolet Communication. Advanced Functional Materials, 2022, 32, .	14.9	20
247	Fabrication, structural characterization, and photoluminescence of Ga-doped ZnO nanobelts. Applied Physics A: Materials Science and Processing, 2009, 94, 799-803.	2.3	19
248	Numerical simulation of the temperature fields of stainless steel with different roller parameters during twin-roll strip casting. International Journal of Minerals, Metallurgy and Materials, 2009, 16, 304-308.	4.9	19
249	Tuning of electronic transport characteristics of ZnO micro/nanowire piezotronic Schottky diodes by bending: threshold voltage shift. Physical Chemistry Chemical Physics, 2010, 12, 14868.	2.8	19
250	Synthesis and transverse electromechanical characterization of single crystalline ZnO nanoleaves. Physical Chemistry Chemical Physics, 2010, 12, 552-555.	2.8	19
251	Facile fabrication of large-scale patterned ZnO nanorod arrays with tunable arrangement, period and morphology. CrystEngComm, 2013, 15, 8022.	2.6	19
252	Enhancing sensitivity of force sensor based on a ZnO tetrapod by piezo-phototronic effect. Applied Physics Letters, 2013, 103, .	3.3	19

#	Article	IF	CITATIONS
253	Single ZnO nanotetrapod-based sensors for monitoring localized UV irradiation. Nanoscale, 2013, 5, 5981.	5.6	19
254	Genetic and epigenetic susceptibility of airway inflammation to PM2.5 in school children: new insights from quantile regression. Environmental Health, 2017, 16, 88.	4.0	19
255	Walnut Polyphenol Extract Protects against Malathion- and Chlorpyrifos-Induced Immunotoxicity by Modulating TLRx-NOX-ROS. Nutrients, 2020, 12, 616.	4.1	19
256	High intensity, plasma-induced emission from large area ZnO nanorod array cathodes. Physics of Plasmas, 2008, 15, 114505.	1.9	18
257	Recycled poly(ethylene terephthalate)/linear lowâ€density polyethylene blends through physical processing. Journal of Applied Polymer Science, 2009, 114, 1187-1194.	2.6	18
258	Stability improvement of the ZnO nanowire array electrode modified with Al2O3 and SiO2 for dye-sensitized solar cells. Materials Letters, 2012, 70, 177-180.	2.6	18
259	A bio-based coating onto the surface Populus fiber for oil spillage cleanup applications. Industrial Crops and Products, 2017, 98, 38-45.	5.2	18
260	One-dimensional ZnO nanostructure-based optoelectronics. Chinese Physics B, 2017, 26, 118102.	1.4	18
261	The comparison of ZnO nanowire detectors working under two wavelengths of ultraviolet. Solid State Communications, 2011, 151, 1860-1863.	1.9	17
262	Numerical simulation on the stress field of austenite stainless steel during twin-roll strip casting process. Computational Materials Science, 2012, 52, 61-67.	3.0	17
263	Photoluminescence and highly selective photoresponse of ZnO nanorod arrays. Optical Materials, 2013, 35, 1532-1537.	3.6	17
264	An enzymatic biosensor based on three-dimensional ZnO nanotetrapods spatial net modified AlGaAs/GaAs high electron mobility transistors. Applied Physics Letters, 2014, 105, .	3.3	17
265	Third-order elastic constants of ZnO and size effect in ZnO nanowires. Journal of Applied Physics, 2014, 115, 213516.	2.5	17
266	Microclimate in an urban park and its influencing factors: a case study of Tiantan Park in Beijing, China. Urban Ecosystems, 2021, 24, 767-778.	2.4	17
267	Room temperature negative differential resistance based on a single ZnO nanowire/CuPc nanofilm hybrid heterojunction. Applied Physics Letters, 2010, 97, 263118.	3.3	16
268	Improvement of the performance and stability of the ZnO nanoparticulate film electrode by surface modification for dye-sensitized solar cells. Colloids and Surfaces A: Physicochemical and Engineering Aspects, 2011, 386, 179-184.	4.7	16
269	The Application of Fluorescence In Situ Hybridization in Different Ploidy Levels Cross-Breeding of Lily. PLoS ONE, 2015, 10, e0126899.	2.5	16
270	Illumination-dependent free carrier screening effect on the performance evolution of ZnO piezotronic strain sensor. Nano Research, 2016, 9, 1091-1100.	10.4	16

#	Article	IF	CITATIONS
271	Impact of insulator layer thickness on the performance of metal–MgO–ZnO tunneling diodes. Nano Research, 2016, 9, 1290-1299.	10.4	16
272	Highly conductive and stretching-insensitive films for wearable accurate pressure perception. Chemical Engineering Journal, 2022, 429, 132488.	12.7	16
273	Crystallization and Mechanical Properties of Recycled Poly(ethylene terephthalate) Toughened by Styrene–Ethylene/Butylenes–Styrene Elastomer. Journal of Polymers and the Environment, 2010, 18, 647-653.	5.0	15
274	Localized ultraviolet photoresponse in single bent ZnO micro/nanowires. Applied Physics Letters, 2010, 97, 133112.	3.3	15
275	Enzymatic lactic acid sensing by In-doped ZnO nanowires functionalized AlGaAs/GaAs high electron mobility transistor. Sensors and Actuators B: Chemical, 2015, 212, 41-46.	7.8	15
276	Ultra-stable ZnO nanobelts in electrochemical environments. Materials Chemistry Frontiers, 2021, 5, 430-437.	5.9	15
277	Bicrystalline Zinc Oxide Nanocombs. Journal of Nanoscience and Nanotechnology, 2006, 6, 2566-2570.	0.9	14
278	Tunable channel width of a UV-gate field effect transistor based on ZnO micro-nano wire. RSC Advances, 2014, 4, 18378.	3.6	14
279	Plasma-induced field emission and plasma expansion of carbon nanotube cathodes. Journal Physics D: Applied Physics, 2007, 40, 3456-3460.	2.8	13
280	Controlled growth and field emission properties of zinc oxide nanopyramid arrays. Applied Surface Science, 2007, 253, 8901-8904.	6.1	13
281	Negative differential resistance in PtIr/ZnO ribbon/sexithiophen hybrid double diodes. Applied Physics Letters, 2009, 95, 123112.	3.3	13
282	Temperature-dependent electron transport in ZnO micro/nanowires. Journal of Applied Physics, 2012, 112, .	2.5	13
283	High-throughput fabrication of large-scale highly ordered ZnO nanorod arrays via three-beam interference lithography. CrystEngComm, 2013, 15, 8416.	2.6	13
284	3D graphene foam/ZnO nanorods array mixed-dimensional heterostructure for photoelectrochemical biosensing. Inorganic Chemistry Frontiers, 2018, 5, 364-369.	6.0	13
285	Transcriptional Regulatory Network of GA Floral Induction Pathway in LA Hybrid Lily. International Journal of Molecular Sciences, 2019, 20, 2694.	4.1	13
286	Broadband electromagnetic wave absorption properties and mechanism of MoS ₂ /rGO nanocomposites. Materials Chemistry Frontiers, 2021, 5, 5063-5070.	5.9	13
287	Large-scale synthesis, microstructure and growth mechanism of self-assembled core–shell ZnO/SiOx nanowires. Materials Letters, 2006, 60, 150-153.	2.6	12
288	Preparation and characteristics of transparent p-type ZnO film by Al and N co-doping method. Applied Surface Science, 2008, 254, 4508-4511.	6.1	12

#	Article	IF	CITATIONS
289	Electrical and mechanical coupling nanodamage in single ZnO nanobelts. Applied Physics Letters, 2010, 96, .	3.3	12
290	Investigation on the Mechanism of Nanodamage and Nanofailure for Single ZnO Nanowires under an Electric Field. ACS Applied Materials & Interfaces, 2014, 6, 2344-2349.	8.0	12
291	Polarityâ€Dependent Piezotronic Effect and Controllable Transport Modulation of ZnO with Multifield Coupled Interface Engineering. Advanced Materials Interfaces, 2017, 4, 1600842.	3.7	12
292	All-Solid-State Supercapacitors Based on Flexible Co3O4 Nanoflowers/rGO Nanocomposites. Journal of Electronic Materials, 2018, 47, 5987-5992.	2.2	12
293	Size Independence and Doping Dependence of Bending Modulus in ZnO Nanowires. Crystal Growth and Design, 2009, 9, 1640-1642.	3.0	11
294	Global Reprogramming of Transcription in Chinese Fir (Cunninghamia lanceolata) during Progressive Drought Stress and after Rewatering. International Journal of Molecular Sciences, 2015, 16, 15194-15219.	4.1	11
295	Local irradiation effects of one-dimensional ZnO based self-powered asymmetric Schottky barrier UV photodetector. Materials Chemistry and Physics, 2015, 166, 116-121.	4.0	11
296	The coupling influence of UV illumination and strain on the surface potential distribution of a single ZnO micro/nano wire. Nano Research, 2016, 9, 2572-2580.	10.4	11
297	Ultra-thin, transparent and flexible tactile sensors based on graphene films with excellent anti-interference. RSC Advances, 2017, 7, 30506-30512.	3.6	11
298	Self-powered visualization system by conjunction of photovoltaic effect and contact-electrification. Nano Energy, 2019, 57, 528-534.	16.0	11
299	The coupling effect characterization for van der Waals structures based on transition metal dichalcogenides. Nano Research, 2021, 14, 1734-1751.	10.4	11
300	Intense electron beam emission from carbon nanotubes and mechanism. Journal Physics D: Applied Physics, 2007, 40, 6626-6630.	2.8	10
301	Electric-induced nanodamage in single ZnO nanowires. Journal of Applied Physics, 2009, 105, .	2.5	10
302	Diameter-dependent internal gain in ZnO micro/nanowires under electron beam irradiation. Nanoscale, 2011, 3, 3060.	5.6	10
303	Plasma-induced field emission study of carbon nanotube cathode. Physical Review Special Topics: Accelerators and Beams, 2011, 14, .	1.8	10
304	Oxidation Behavior of Hot Pressed <scp>Z</scp> r <scp>B</scp> ₂ â€ <scp>Z</scp> r <scp>C</scp> â€ <scp>S</scp> i <scp>C</scp> Ceramic Composites. International Journal of Applied Ceramic Technology, 2014, 11, 178-185.	2.1	10
305	A preliminary study on the crossability in Robinia pseudoacacia L. Euphytica, 2015, 206, 555-566.	1.2	10
306	Flexible electronics and optoelectronics of 2D van der Waals materials. International Journal of Minerals, Metallurgy and Materials, 2022, 29, 671-690.	4.9	10

#	Article	IF	CITATIONS
307	Quasi One-dimensional ZnO Nanostructures Fabricated without Catalyst at Lower Temperature. Frontiers of Physics in China, 2006, 1, 72-84.	1.0	9
308	High intensity, plasma-induced electron emission from large area carbon nanotube array cathodes. Applied Physics Letters, 2010, 96, 073109.	3.3	9
309	Surface destruction and performance reduction of the ZnO nanowire arrays electrode in dye sensitization process. Materials Letters, 2011, 65, 3506-3508.	2.6	9
310	Fast sensitization process of ZnO-nanorod-array electrodes by electrophoresis for dye-sensitized solar cells. RSC Advances, 2014, 4, 39332.	3.6	9
311	Nitric Oxide Enhances Cytotoxicity of Lead by Modulating the Generation of Reactive Oxygen Species and Is Involved in the Regulation of Pb2+ and Ca2+ Fluxes in Tobacco BY-2 Cells. Plants, 2019, 8, 403.	3.5	9
312	Thickness and Morphology Dependent Electrical Properties of ALD‣ynthesized MoS ₂ FETs. Advanced Electronic Materials, 2022, 8, .	5.1	9
313	Field-emission properties of individual ZnO nanowires studiedin situby transmission electron microscopy. Journal of Physics Condensed Matter, 2007, 19, 176001.	1.8	8
314	Field emission properties of a carbon nanotube cathode in different electric field modes. Materials Letters, 2008, 62, 1941-1944.	2.6	8
315	Negative differential resistance in ZnO nanowires induced by surface state modulation. Materials Chemistry and Physics, 2011, 131, 258-261.	4.0	8
316	Utilization of electron beam to modulate electron injection over Schottky barrier. Current Applied Physics, 2011, 11, 586-589.	2.4	8
317	Transport Property Tuned by Gate Irradiation in ZnO Nanotetrapod Devices. Journal of Physical Chemistry C, 2012, 116, 12397-12400.	3.1	8
318	Investigation of electron beam detection properties of ZnO nanowire based back-to-back double Schottky diode. RSC Advances, 2014, 4, 12743.	3.6	8
319	Influence of piezoelectric effect on dissolving behavior and stability of ZnO micro/nanowires in solution. RSC Advances, 2015, 5, 3365-3369.	3.6	8
320	An uncertainty-based multivariate statistical approach to predict crop water footprint under climate change: a case study of Lake Dianchi Basin, China. Natural Hazards, 2020, 104, 91-110.	3.4	8
321	Controlling the Facet of ZnO during Wet Chemical Etching Its (0001Â⁻) Oâ€Terminated Surface. Small, 2020, 16, e1906435.	10.0	8
322	Identification of Photoexcited Electron Relaxation in a Cobalt Phosphide Modified Carbon Nitride Photocatalyst. ChemPhotoChem, 2021, 5, 330-334.	3.0	8
323	On the Contact Optimization of ALD-Based MoS ₂ FETs: Correlation of Processing Conditions and Interface Chemistry with Device Electrical Performance. ACS Applied Electronic Materials, 2021, 3, 3185-3199.	4.3	8
324	Surface Energy of In-Doped ZnO Studied by PAW+U Method. Materials Science Forum, 2007, 561-565, 1861-1864.	0.3	7

#	Article	IF	CITATIONS
325	Characterization of Ba1.0Sr1.0FeO4+δ cathode on La0.9Sr0.1Ga0.8Mg0.2O3â~`δ electrolyte for intermediate temperature solid oxide fuel cells. Journal of Power Sources, 2011, 196, 6238-6241.	7.8	7
326	Constitutive Modeling of High-Temperature Flow Behavior of an Nb Micro-alloyed Hot Stamping Steel. Journal of Materials Engineering and Performance, 2016, 25, 948-959.	2.5	7
327	Ultrathin strain-gated field effect transistor based on In-doped ZnO nanobelts. APL Materials, 2017, 5, .	5.1	7
328	Effect of UV Irradiation and Heat Treatment on the Surface Potential Distribution of Monolayer WS ₂ on SiO ₂ /Si and Au Substrates. Advanced Materials Interfaces, 2018, 5, 1701083.	3.7	7
329	Information accessibility oriented self-powered and ripple-inspired fingertip interactors with auditory feedback. Nano Energy, 2021, 87, 106117.	16.0	7
330	Field emission characteristics of ZnO nanotetrapods and the effect of thermal annealing in hydrogen. Science Bulletin, 2007, 52, 1287-1290.	1.7	6
331	Size dependence of transverse electric transport in single ZnO nanoneedles. Applied Physics Letters, 2010, 96, 152101.	3.3	6
332	Effect of ozone adsorption on the oxidation behaviour of ZrB2–SiC ceramic composites. Corrosion Science, 2011, 53, 840-844.	6.6	6
333	Defects Energetics and Electronic Properties of Li Doped ZnO: A Hybrid Hartree-Fock and Density Functional Study. Chinese Journal of Chemical Physics, 2012, 25, 261-268.	1.3	6
334	Study on the Electron Emission Properties of ZnO Nanorod Arrays on Different Substrates. Journal of Nanoscience and Nanotechnology, 2012, 12, 775-780.	0.9	6
335	Influences of low temperature thermal treatment on ZnO nanowire arrays and nanoparticles based flexible dye-sensitized solar cells. Colloids and Surfaces A: Physicochemical and Engineering Aspects, 2012, 402, 127-131.	4.7	6
336	AFM investigation of nanomechanical properties of ZnO nanowires. RSC Advances, 2015, 5, 33445-33449.	3.6	6
337	Triboelectricity-assisted transfer of graphene for flexible optoelectronic applications. Nano Research, 2016, 9, 899-907.	10.4	6
338	Enhanced sulfur utilization in lithium-sulfur batteries by hybrid modified separators. Materials Today Communications, 2021, 26, 102133.	1.9	6
339	Effects of individual and community-level environment components on the subjective well-being of poverty alleviation migrants: the case in Guizhou, China. International Journal of Sustainable Development and World Ecology, 2021, 28, 622-631.	5.9	6
340	Abnormal magnetic behavior in DMS Zn1â^'x MnxO nanowires. Science Bulletin, 2006, 51, 490-492.	1.7	5
341	Morphological effects on the plasma-induced emission properties of large area ZnO nanorod arrays. Journal Physics D: Applied Physics, 2009, 42, 215203.	2.8	5
342	Fabrication and Optical Properties of Mn-Doped ZnO Nanowires. Advanced Materials Research, 2009, 79-82, 453-456.	0.3	5

#	Article	IF	CITATIONS
343	Influence of electromechanical coupling and electron irradiation on the conductivity of individual ZnO nanowire. Solid State Sciences, 2011, 13, 658-661.	3.2	5
344	Effect of modified carbon black on the UV/IR screening ability of poly(ethylene terephthalate) transparent films. Polymer Composites, 2011, 32, 297-304.	4.6	5
345	Tuning electronic transport of ZnO micro/nanowires by a transverse electric field. Applied Physics Letters, 2011, 99, 063105.	3.3	5
346	Two-step epitaxial synthesis and layered growth mechanism of bisectional ZnO nanowire arrays. Journal of Crystal Growth, 2013, 363, 247-252.	1.5	5
347	Dissolving behavior and electrical properties of ZnO wire in HCl solution. RSC Advances, 2015, 5, 44563-44566.	3.6	5
348	Hormonal Regulatory Patterns of LaKNOXs and LaBEL1 Transcription Factors Reveal Their Potential Role in Stem Bulblet Formation in LA Hybrid Lily. International Journal of Molecular Sciences, 2021, 22, 13502.	4.1	5
349	Nonisothermal crystallization behavior and UV screening ability of poly(ethylene) Tj ETQq1 1 0.784314 rgBT /O	verlgck 10) Tf 50 502 T
350	Mechanical properties and indentation-induced damage of high-quality ZnO microwires. Materials Research Bulletin, 2012, 47, 750-754.	5.2	4
351	First-principles studies on transport properties and contact effects of Cu(111)/ZnO-nanobelt(101̄0)/Cu(111) systems. Physical Chemistry Chemical Physics, 2013, 15, 13070.	2.8	4
352	First-principles study on the effect of high In doping on the conductivity of ZnO. Chinese Physics B, 2013, 22, 077103.	1.4	4
353	3D stress simulation and parameter design during twin-roll casting of 304 stainless steel based on the Anand model. International Journal of Minerals, Metallurgy and Materials, 2014, 21, 666-673.	4.9	4
354	Strain-modulated transport properties of Cu/ZnO-nanobelt/Cu nanojunctions. Physica Status Solidi (B): Basic Research, 2015, 252, 1767-1772.	1.5	4
355	Synthesis of edge-enriched WS2 on high surface area WS2 framework by atomic layer deposition for electrocatalytic hydrogen evolution reaction. Journal of Vacuum Science and Technology A: Vacuum, Surfaces and Films, 2020, 38, .	2.1	4
356	Comparative Genomic Analysis Reveals the Mechanism Driving the Diversification of Plastomic Structure in Taxaceae Species. Frontiers in Genetics, 2019, 10, 1295.	2.3	4
357	Increased abscisic acid sensitivity and drought tolerance of Arabidopsis by overexpression of poplar abscisic acid receptors. Plant Cell, Tissue and Organ Culture, 2022, 148, 231-245.	2.3	4
358	The transcription factor GNC optimizes nitrogen use efficiency and growth by up-regulating the expression of nitrate uptake and assimilation genes in poplar. Journal of Experimental Botany, 2022, 73, 4778-4792.	4.8	4
359	Evaluation of nano-structured Ir0.5Mn0.5O2 as a potential cathode for intermediate temperature solid oxide fuel cell. Journal of Power Sources, 2008, 185, 946-951.	7.8	3
360	Investigation on the Plasma-Induced Emission Properties of Large Area Carbon Nanotube Array Cathodes with Different Morphologies. Nanoscale Research Letters, 2011, 6, 40.	5.7	3

#	Article	IF	CITATIONS
361	Combined Field and Thermionic Emission Process in ZnO Nanostructure Cold Emission Cathode. Materials Science Forum, 2010, 654-656, 1138-1141.	0.3	3
362	Multi-zone light emission in a one-dimensional ZnO waveguide with hybrid structures. Optical Materials Express, 2011, 1, 173.	3.0	3
363	Electron irradiation effect on the Schottky gate of ZnO nanowires-based field effect transistors. Micro and Nano Letters, 2011, 6, 437.	1.3	3
364	Mechanical properties of Mn-doped ZnO nanowires studied by first-principles calculations. International Journal of Minerals, Metallurgy and Materials, 2012, 19, 89-94.	4.9	3
365	Nonlinear elastic response of cubic crystals to biaxial strain. Computational Materials Science, 2013, 79, 284-288.	3.0	3
366	Determinants of Children's Exhaled Nitric Oxide: New Insights from Quantile Regression. PLoS ONE, 2015, 10, e0130505.	2.5	3
367	Enhanced electromechanical performance in metal–MgO–ZnO tunneling diodes due to the insulator layers. Inorganic Chemistry Frontiers, 2016, 3, 1130-1136.	6.0	3
368	Seasonal expressions of prostaglandin E synthases and receptors in the prostate of the wild ground squirrel (Spermophilus dauricus). Prostaglandins and Other Lipid Mediators, 2020, 148, 106412.	1.9	3
369	Both Clathrin-Mediated and Membrane Microdomain-Associated Endocytosis Contribute to the Cellular Adaptation to Hyperosmotic Stress in Arabidopsis. International Journal of Molecular Sciences, 2021, 22, 12534.	4.1	3
370	Zinc Powder Evaporation: an Efficient Way of Synthesizing a Wide Range of High-quality ZnO Nanostructures at Lower Temperature. Materials Research Society Symposia Proceedings, 2005, 872, 1.	0.1	2
371	Electromagnetic Wave Absorption Properties of Nanoscaled ZnO. , 0, , .		2
372	Asymmetric Behavior in Flexible Piezoelectric Strain Sensors Made of Single ZnO Nanowires. Journal of Nanoscience and Nanotechnology, 2014, 14, 6084-6088.	0.9	2
373	Morphology and Properties of Tetraleg ZnO Nanostructures Fabricated by Zn-Powder Evaporation without Catalysts at Lower Temperature. Materials Research Society Symposia Proceedings, 2005, 879, 1.	0.1	1
374	A quantum explanation of the abnormal magnetic behaviour in Mn-doped ZnO nanowires. Journal of Physics Condensed Matter, 2007, 19, 236223.	1.8	1
375	Study on Curing Behavior of Low Molar Ratio Urea-Formaldehyde Resins with Different Curing Agents. Advanced Materials Research, 2010, 150-151, 965-968.	0.3	1
376	Fabrication and electrical property of individual ZnO nanowire based mesfet. Procedia Engineering, 2012, 27, 1471-1477.	1.2	1
377	Calibration on force upon the surface of single ZnO nanowire applied by AFM tip with different scanning angles. RSC Advances, 2015, 5, 47309-47313.	3.6	1
378	A cross-contamination risk assessment model with improved coefficient optimization for Campylobacter. International Journal of Food Properties, 2020, 23, 1579-1596.	3.0	1

#	Article	IF	CITATIONS
379	Tuning drought resistance by using a root-specific expression transcription factor PdNF-YB21 in Arabidopsis thaliana. Plant Cell, Tissue and Organ Culture, 2021, 145, 379-391.	2.3	1
380	Highly Oriented Plate-like Rod/Tube Arrays of ZnO. Materials Research Society Symposia Proceedings, 2005, 876, 1.	0.1	0
381	Three-Dimensional Zinc Oxide Nanorod Networks. Advanced Materials Research, 2009, 79-82, 457-460.	0.3	0
382	Mechanical Properties and Size Effects of ZnO Nanowires Studied by First-Principles Calculation. Materials Science Forum, 2010, 654-656, 1670-1673.	0.3	0
383	Investigation on the Plasma-Induced Electron Emission Properties of ZnO Nanorod and Carbon Nanotube Arrays. Materials Science Forum, 2010, 654-656, 1150-1153.	0.3	0
384	Current Steps in Poly(3-Hexylthiophene)/ZnO Nanobelt Hybrid Diodes. Materials Science Forum, 2010, 654-656, 1158-1161.	0.3	0
385	The Electrical Characterization of Single ZnO Nanowries Field-Effect Transistors. Materials Science Forum, 2010, 654-656, 1178-1181.	0.3	0
386	Fabrication and Optical Properties of Mn Doped ZnS Nanowires. Advanced Materials Research, 0, 236-238, 2211-2215.	0.3	0
387	DOPING EFFECT OF THE ELECTRONIC TRANSPORT PROPERTIES OF ZINC OXIDES NANOWIRES STUDIED BY FIRST PRINCIPLES CALCULATION. , 2012, , .		0
388	Active Flexible Strain Sensor Based on Single ZnO Micro/Nanowire. Materials Research Society Symposia Proceedings, 2013, 1556, 1.	0.1	0
389	Enhanced Field Emission Characteristics of ZnS Dentalation Nanostructures. Advanced Materials Research, 2014, 936, 379-383.	0.3	0
390	Size Effect of Piezoelectricity in ZnO Nanowires: A First-Principles Study. Key Engineering Materials, 0, 645-646, 275-280.	0.4	0
391	One-dimensional ZnO Nanomaterials Based Electronics and Sensing Devices. , 2013, , .		0
392	Application of ZnO Nanowires in Solar Energy Conversion. , 2015, , .		0